Scientific Research

Modified Bow-Tie Nanoparticles Operating in the Visible and Near Infrared Frequency Regime

Renato Iovine, Luigi La Spada, Lucio Vegni

Department of Applied Electronics, "Roma Tre" University, Rome, Italy
Email: renato.iovine@uniroma3.it, luigi.laspada@uniroma3.it, vegni@uniroma3.it

ABSTRACT

In this contribution electromagnetic properties of traditional and modified bow-tie nanoparticles are investigated. The modified bow-tie particles consist of a pair of opposing metallic truncated triangles, embedded in a dielectric environment, with a rectangular dielectric hole engraved on the metallic structure. New analytical models for both structures are developed in order to describe the nanoparticles electromagnetic behavior in terms of resonant wavelength position, magnitude and amplitude width for the extinction cross-section. Analytical results are compared to the numerical values and to the experimental ones existing in literature. Good agreement among them is obtained. Then, the structures are analyzed in terms of sensitivity properties. Results reveal that the modified bow-tie structure can be applied for bio-medical applications.

1. Introduction

In the last few years several researchers have been involved in nanoparticle-based devices development, paving the way for new biomedical applications.

Metallic nanoparticles exhibit unusual optical properties deriving from the strong local electromagnetic field enhancement in the neighborhood of the structure under the Localized Surface Plasmon Resonance (LSPR) excitation [1].

As a result the interaction between the localized electromagnetic field and the surrounding dielectric environment is restricted in a small area. Therefore, such structures are very sensitive to changes in the refractive index of the surrounding dielectric medium.

Most of biomedical applications, based on nanoparticles, exploit the interaction between the electromagnetic field with metal nanoparticles in the Visible (VIS) and Near Infrared Region (NIR) [2]. These electromagnetic properties make metallic nanoparticles suitable for several application fields: such as biochemical sensing and detection [3,4], protein analysis [5,6], cell membrane function [7], food quality analysis [8]. They can also be used as contrast agents in cellular and biological imaging [9, 10], Raman signal intensity enhancement [11,12] and therapeutic applications as photo thermal destruction of cancerous cells [13].

The nanoparticle effectiveness as sensing or therapeutic tool depends on its optical properties. In particular, it

is well known that smaller particles are excellent absorbers; and on the contrary the bigger ones are very strong scatters [14].

Although several researches have focalized the attention on the experimental evaluation of nanoparticle electromagnetic characteristics (in terms of wavelength position, magnitude and bandwidth), little is known about the possibility to control the physical phenomenon. Predicting the electromagnetic behavior of such structures is of considerable interest to build up inclusions that satisfy certain requirements, for specific applications.

In this regard, this paper attempts to present a new design method for bow-tie-based nanoparticles.

These particles (a pair of opposing gold truncated triangles) are used in order to obtain the strong hot spot in their gap. In fact, the possibility to tune the structure response by varying its geometrical parameters such as bow-tie angle, side length and gap distance has been studied [15,16]. The effects of the bow-tie geometry on its sensitivity have been recently evaluated [17]. Such results suggest that bow-tie nanoparticles can be employed for sensing applications. Despite this, the literature is almost silent on the development of models useful to design such structures.

For this reason, in this paper new analytical models are presented.

Moreover, in this study we propose modified bow-tie particles by using a dielectric rectangular hole engraved on the structure. In this configuration nanoparticles ex-

hibit a multi resonant behavior associated with a high electric field localizations (hot spots) near the nanoparticles.

The main advantage in using analytical models is the possibility to tune the nanostructure resonances, in the VIS and NIR frequency regime, by changing its geometrical and electromagnetic properties.

The article is structured as follows:

- First of all, the electromagnetic properties of a classical bow-tie nanoparticle are evaluated in terms of extinction cross-section. A new analytical model, describing its electromagnetic resonant behaviour in terms of wavelength position, magnitude and bandwidth, is proposed. In order to validate the proposed closed-form formula, a comparison among analytical, numerical and experimental values is shown.
- Secondly, by introducing a dielectric hole in the bow-tie particle, an additional hot spot and a multi resonant behavior were obtained. The effect of the dielectric hole, on the particle electromagnetic behavior, is analytically described.
- Then, the effects of geometrical and electromagnetic parameters on the resonant properties for both structures are explored.
- Finally, the sensitivity of the traditional and modified bow-tie particles are evaluated and discussed. A comparison between the sensitivity of the traditional bow-tie and the modified one is proposed.

2. Analytical Models and Electromagnetic Properties of Bow-Tie Nanoparticles

In this section, the electromagnetic properties for the classical bow-tie geometry and the modified one are presented. The aim is to present a new design method to build up the aforementioned nanoparticles with desired electromagnetic properties.

The proposed geometries consist of a pair of opposing metallic truncated triangles embedded in a dielectric environment. The structure is excited by a plane-wave, having the electric field **E** parallel and the propagation vector **k** perpendicular to the plane containing the particle as depicted in **Figure 1**. Specifically, the nanostructure optical properties in terms of extinction cross-sections (C_{ext}) and the electric field distribution (hot spots) at the resonant wavelength are evaluated.

The considered geometrical parameters are shown in **Figure 1**. They are: the major-side length a, the height of the triangles b, the minor-side length c, the inter-particles gap d, the height of the dielectric hole g, the minor-side of the dielectric hole f and the thickness e of the structures.

In order to study their resonant properties the following assumptions are stated:

- The particle sizes are much smaller than the operative wavelength [18]. In this way, inclusions can be considered "electrically small". Therefore their resonant behavior can be studied in terms of quasi-static approximation;
- The particle is homogeneous and the surrounding dielectric environment is a homogeneous and non-absorbing medium.

Under such conditions, we can relate the electromagnetic extinction properties of the nanoparticle to its polarizability expression.

Let's point out some relevant aspects concerning the present work:

- For metallic nanoparticles, experimental values [19] of the complex permittivity function have been used;
- The surrounding dielectric medium is considered to be vacuum.

2.1. Bow-Tie Analytical Model and Electromagnetic Properties

In case of arbitrary shaped particles, the dipolar polarizability expression reads [18]:

$$\alpha = V\varepsilon_e \frac{\varepsilon_i - \varepsilon_e}{\varepsilon_e + L(\varepsilon_i - \varepsilon_e)} \quad (1)$$

where V is the particle volume, ε_e is the electric permittivity of the surrounding dielectric environment, ε_i is the inclusion electric permittivity and L is the depolarization factor. Following the same procedure conducted in [20], it is possible to develop new analytical models describing the extinction cross-section properties for both considered nanoparticles. The general corresponding expression can be written as follows:

$$C_{ext} = k \cdot Im[\alpha] + \frac{k^4}{6\pi}|\alpha|^2 \quad (2)$$
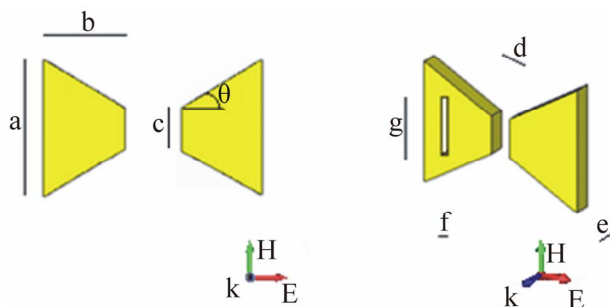
Figure 1. Geometrical sketch of the particles under study: (a) Top view of classical bow-tie particle; (b) Perspective view of modified bow-tie particle by dielectric incision. Geometrical parameters: $a = 2b\tan\theta + c$; $b = 100$ nm; $c = 50$ nm; $d = 20$ nm; $e = 25$ nm; $10 \le f \le 30$; $80 \le g \le 100$; $30° \le \theta \le 60°$.

where $k = \dfrac{2\pi n}{\lambda}$ is the wave number, λ is the wavelength and $n = \sqrt{\varepsilon_e}$ is the refractive index of the surrounding dielectric environment.

Considering such elements and the electric field polarization of the impinging plane wave, the polarizability formula for the classical bow-tie particle follows:

$$\alpha_1 = \frac{1}{3} e \big(a (2b+d) - cd \big) \frac{\varepsilon_e (\varepsilon_i - \varepsilon_e)}{\varepsilon_e + L_1 (\varepsilon_i - \varepsilon_e)} \qquad (3)$$

with

$$L_1 = \frac{3}{\pi} \tan^{-1} \left[\frac{a \cdot e}{\left(b + \dfrac{d}{2} \right) \sqrt{a^2 + 4 \left(b + \dfrac{d}{2} \right)^2 + e^2}} \right] \qquad (4)$$

In **Figure 2** a comparison between analytical model and numerical simulation, performed by the full-wave solver CST Microwave studio [21], for the extinction cross-section spectra of gold traditional bow-tie nanoparticle is shown.

In our simulations we have used a time-domain method based on finite integration technique (FIT). In particular, the structure is discretized using hexagonal mesh. To make sure that the particles are represented as well as possible, we have optimized the Global Mesh Properties parameters (lines per wavelength: 30; lower mesh limit: 30; mesh line ratio limit: 10) and used a Mesh refinement process (local edge refinement factor: 6; local volume refinement factor: 4). The final mesh consisted of around 2,000,000 mesh elements depending on the geometrical parameters.

In order to verify the quality of the proposed model, analytical results are compared to the numerical values and to the experimental ones [15,22], for different geometrical parameter dimensions, as reported in **Table 1**.

The relative errors were evaluated and reported in **Table 1**. Good agreement among all the three results was achieved.

2.2. Modified Bow-Tie Analytical Model and Multi-Resonant Properties

Until now inclusions have been assumed to be homogeneous structures.

In this section a new non homogeneous structure is proposed. The classical bow-tie structure is modified by inserting a dielectric hole in one of its side, as shown in **Figure 1(b)**.

The reason for the employment of the dielectric hole in the classical bow-tie particle is the possibility to excite a new resonant frequency on the same structure in order to achieve a multi-band behavior.

The main advantages to use a multi-resonant structure

are the following:

- Improved sensor sensitivity: the excitation of multiple resonant frequencies in the same structure, caused by such a configuration, leads to a high electromagnetic field localization in the neighbourhood of the nanoparticles (an additional hot spot is obtained). By using the dielectric hole (perpendicular to the electric field oscillation axis) inside the bow-tie particle, an additional resonant peak is obtained as shown in **Figure 3**. From a physical point of view, the multi-resonant behavior can be related to the additional capacitance existing inside the particle. This resonance is localized towards longer wavelengths compared to the classical bow-tie configuration (**Figure 3**) due to the fact that we have assumed $g > c$ as shown in **Figure 1**.

- The possibility to tune the nanostructure resonances, by changing its geometrical and electromagnetic characteristics in order to coincide with the spectral absorption characteristics of the sample is under study. It turns out to be a useful tool for absorption measurements.

In particular, by following the same procedure conducted in the previous section, in order to control and to tune such frequencies a new analytical model for the
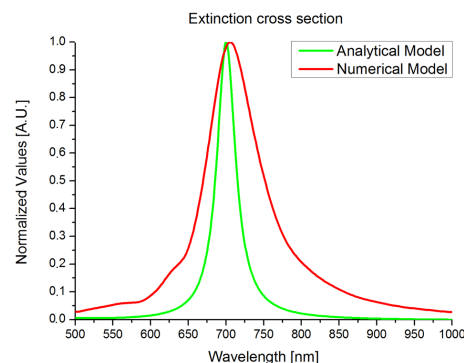
Figure 2. Analytical-numerical model comparison for the extinction cross-section spectra for gold classical bow-tie nanoparticle: $\theta = 30°$.
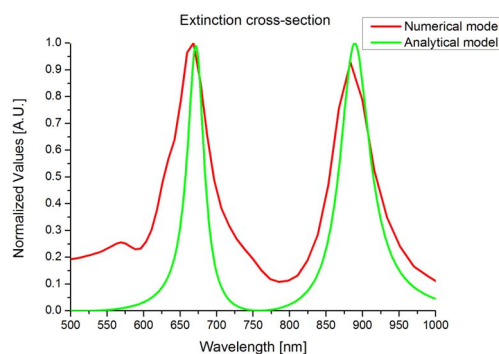
Figure 3. Analytical-numerical model comparison for the extinction cross-section spectra for gold modified bow-tie nanoparticles: $f = 10$ nm, $g = 80$ nm and $\theta = 30°$.

modified bow-tie polarizability was developed. In this case the total polarizability is the sum of the traditional bow-tie polarizability α_1 and the dielectric hole polarizability α_2 as follows

$$\alpha_{tot} = \alpha_1 + \alpha_2 \qquad (5)$$

being:

$$\alpha_2 = \frac{e \cdot f \cdot g \cdot \varepsilon_e \left(\varepsilon_i - \varepsilon_e \right)}{\varepsilon_e + L_2 \left(\varepsilon_i - \varepsilon_e \right)} \qquad (6)$$

with

$$L_2 = \frac{1}{3\pi} \left(1 - \frac{g}{\sqrt{16e^2 + g^2}} \right) \text{Sinc} \left(\sqrt{\frac{2}{5} \frac{f}{g}} + 1 \right) \qquad (7)$$

A comparison between analytical and numerical models for the extinction cross-section spectra is shown in **Figure 3**.

This electromagnetic behavior is also confirmed by full-wave numerical simulations. Considering a modified bow-tie with the following geometrical parameters for the dielectric hole: $f = 10$ nm and $g = 80$ nm the electric field distribution in the nanoparticle is shown in **Figures 4** and **5**. It can be noted that the electric field localization inside the dielectric hole (**Figure 4**) leads to a new resonant peak (883 nm), while the electric field distribution existing in the gap (**Figure 5**) represents the resonant frequency (668 nm) that can be found in the classical bow-tie configuration.

3. Effect of the Geometrical and Electromagnetic Parameters

The inclusion electromagnetic properties are highly dependent on the size, shape, and nanoparticle composition. Therefore, in this section the effect of the geometrical and electromagnetic parameters on the nanoparticle resonant behavior is studied. In order to design the aforementioned inclusions, we relate their electromagnetic resonant properties to the geometrical parameters, to the metallic material properties (real and imaginary part of permittivity: ε_{real} and ε_{imm}, respectively), and to the surrounding dielectric environment permittivity ε_e. It is well known that the particle polarizability is at its resonant condition when:

$$\left[\varepsilon_e + L \left(\varepsilon_i - \varepsilon_e \right) \right] = 0 \qquad (8)$$

Assuming that the inclusion permittivity can be expressed as $\varepsilon_i = \varepsilon_{ireal} + j\varepsilon_{iimm}$ and the background material permittivity as $\varepsilon_e = \varepsilon_{ereal} + j\varepsilon_{eimm}$ the particle resonant condition (in the quasi-static approximation) occurs at:

$$\varepsilon_{ireal} = \frac{(L-1)L\varepsilon_{ereal} - \sqrt{-L^2 \left((L-1)\varepsilon_{eimm} - L\varepsilon_{iimm} \right)^2}}{L^2} \qquad (9)$$
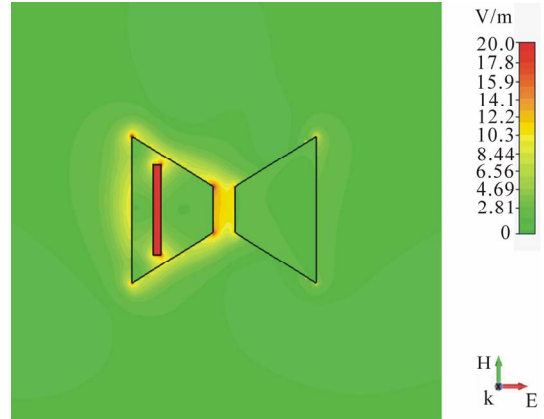
Figure 4. Near electric field distribution of modified bow-tie particle with $\theta = 30°$; $f = 10$ nm, $g = 80$ nm at 883 nm.
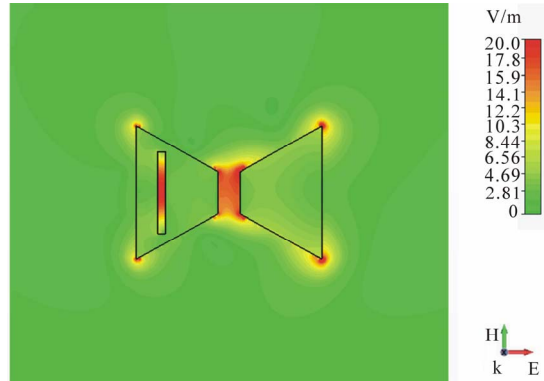
Figure 5. Near electric field distribution of modified bow-tie particle with $\theta = 30°$; $f = 10$ nm, $g = 80$ nm at 668 nm.

Then the role of the geometrical parameters, on the bow-tie particle resonant behavior can be evaluated. By using (9) and assuming a background lossless material ($\varepsilon_{eimm} = 0$) the traditional bow-tie particle resonant condition reads:

$$\varepsilon_{ireal1} = \left(1 - \frac{\pi}{3\text{ArcTan}\left(\frac{a \cdot e}{(2b+d)\sqrt{a^2 + (2b+d)^2 + e^2}} \right)} \right) \times \varepsilon_{ereal} - \varepsilon_{iimm} \qquad (10)$$

An example of the effects of the geometrical parameters variations on bow-tie resonant properties is shown in **Figure 6**.

Let's now consider the modified bow-tie particle. A similar expression for the resonant condition can be obtained. In this case we have two coexisting solutions. The first resonant condition was reported before and it refers to the traditional bow-tie resonance-see (10). The second

Table 1. Comparison of resonant wavelengths for classical bow-tie particle: analytical, numerical and experimental values (silver [15]: $a = 2b\tan[\theta] + c$, $b = 140$ nm, $c = 5$ nm, $d = 28.5$ nm, $e = 48$ nm; gold [22]: $a = 2b\tan[\theta] + c$, $c = 5$ nm, $d = 12$ nm, $e = 20$ nm, $\theta = 28°$).

Nanoparticle geometry	Size [nm]	Resonant wavelength (λ [nm])			Analytical-numerical error (%) $\dfrac{\lambda_{analytical} - \lambda_{numerical}}{\lambda_{numerical}}$	Analytical-experimental error (%) $\dfrac{\lambda_{analytical} - \lambda_{experiental}}{\lambda_{experiental}}$
		Analytical values	Numerical values	Experimental values [15,22]		
Silver [15]	$\theta = 10°$	810	815	825	0.613	1.818
	$\theta = 20°$	820	824	830	0.606	1.205
	$\theta = 30°$	860	853	850	0.5848	1.1765
Gold [22]	$b = 75$	700	704	710	0.568	1.408
	$b = 90$	750	753	760	0.398	1.316
	$b = 100$	780	784	790	0.51	1.266

resonant condition (corresponding to the dielectric hole resonant behavior) reads:

$$\varepsilon_{ireal2} = \frac{\varepsilon_{ereal}}{16e^2\text{Sinc}\left(\sqrt{\dfrac{2}{5}\dfrac{f}{g}}+1\right)}\left(16e^2\text{Sinc}\left(\sqrt{\dfrac{2}{5}\dfrac{f}{g}}+1\right)\right.$$
$$\left. -3\pi\left(g\left(\sqrt{16e^2 + g^2}+g\right)+16e^2\right)\right) - \varepsilon_{iimm} \quad (11)$$

By varying the geometrical parameters of the dielectric hole it is possible to tune the position, magnitude and amplitude width of the additional resonant peak as shown in **Figures 7** and **8**.

4. Sensitivity Analysis and Performances

In this section we analyze the sensitivity properties of both bow-tie nanoparticles. The sensitivity is commonly defined as the ratio wavelength shift to refractive index variation, expressed in nm/RIU (Refractive Index Unit). The sensitivity performances in the range $1 < n < 1.6$ for different geometrical parameters of the traditional bow-tie and the modified one have been evaluated (**Tables 2** and **3**).

In particular, in **Table 2** a comparison for the traditional bow-tie among analytical, numerical and experimental values [23,24] is reported.

Instead, in **Table 3** the sensitivity performances for the modified bow-tie particle, as a function of f and g values, are shown.

The following relevant aspects can be pointed out:

First of all, the introduction of the dielectric hole leads to higher sensitivities values compared to the traditional configuration for the first resonant peak (compared to the traditional bow-tie particle).

Secondly, the sensitivity of the first LSPR peak (■) is small influenced by varying the geometrical parameters
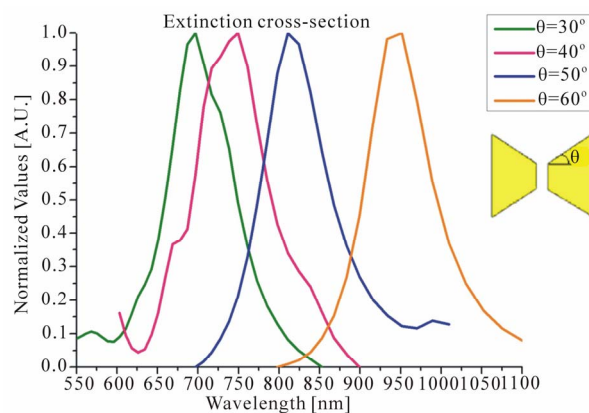
Figure 6. Extinction spectra of classical bow-tie particles by varying θ.
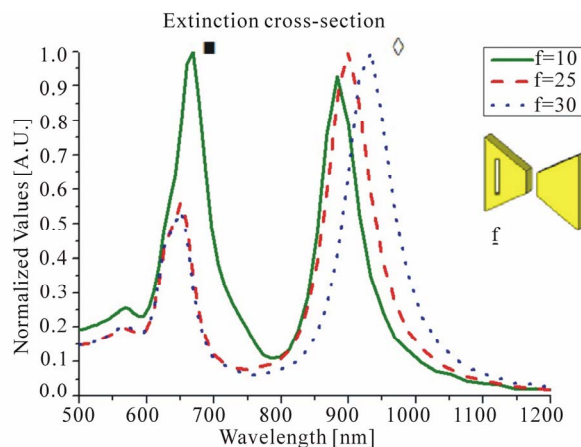
Figure 7. Extinction spectra of modified bow-tie particle by varying dielectric incision geometry: 10 nm $< f <$ 30 nm, $\theta = 30°$, $g = 80$ nm.

of the dielectric hole. On the other hand, the new resonant peak (◊), related to the hole, is strongly influenced by such variations. In particular it is possible to observe

Table 2. Sensitivity values for traditional bow-tie particles.

Traditional Bow-tie	Sensitivity [nm/RIU]		
	Analytical sensitivity	Numerical sensitivity	Experimental sensitivity [23,24]
Silver [23]	220	210	203
Gold [24]	210	205	200

Table 3. Sensitivity performances of modified bow-tie particles for different value of *f* and *g*.

Geometrical parameters: $a = 2b\tan\theta + c$ $b = 100$ nm; $c = 50$ nm; $d = 20$ nm; $e = 25$ nm; $\theta = 30$.	Size (nm)	Resonant wavelength λ [nm]				Mean sensitivity values [nm/RIU]
		$n = 1$	$n = 1.2$	$n = 1.4$	$n = 1.6$	
$g = 80$ nm; $f = 10$ nm.	■	668	749	852	951	471
	◊	883	1034	1180	1336	755
$g = 85$ nm; $f = 10$ nm.	■	664	755	855	968	506
	◊	920	1073	1235	1374	756
$g = 90$ nm; $f = 10$ nm.	■	668	760	853	952	473
	◊	960	1136	1295	1455	825
$g = 95$ nm; $f = 10$ nm.	■	668	762	856	958	511
	◊	1009	1180	1347	1534	875
$g = 100$ nm; $f = 10$ nm.	■	668	762	875	975	511
	◊	1051	1234	1416	1585	890
$g = 80$ nm; $f = 15$ nm.	■	659	738	836	932	455
	◊	869	1007	1174	1300	718
$g = 80$ nm; $f = 20$ nm.	■	652	738	825	919	445
	◊	883	1029	1180	1339	760
$g = 80$ nm; $f = 25$ nm.	■	652	727	825	913	435
	◊	900	1053	1207	1372	786
$g = 80$ nm; $f = 30$ nm.	■	652	729	820	916	440
	◊	932	1094	1240	1413	801

that sensitivity performances grow by increasing the hole length *g*.

The following bow-tie configuration: $a = 2b\tan\theta + c$; $b = 100$ nm; $c = 50$ nm; $d = 20$ nm; $e = 25$ nm; $\theta = 30°$; $g = 100$ nm; $f = 10$ nm exhibits good value of sensitivity for the LSPR peaks (■ 511 nm/RIU and ◊ 890 nm/RIU). Such a result is confirmed by the analytical model and numerical simulations, suggesting the possibility to use the modified bow-tie structure for sensing applications.
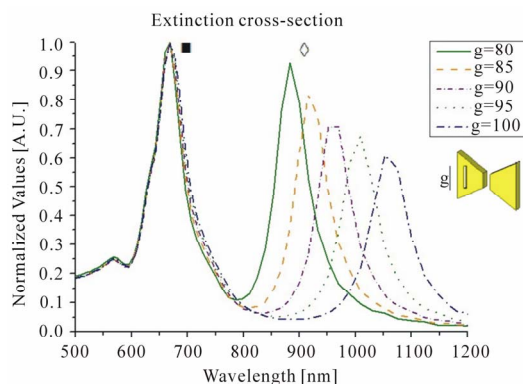
Figure 8. Extinction spectra of modified bow-tie particle by varying dielectric incision geometry: 80 nm < *g* < 100 nm, $\theta = 30°$, *f* = 10 nm.

5. Conclusions

In this contribution electromagnetic properties of traditional and modified bow-tie particles in the Infrared and Visible frequency range were investigated.

New closed-form analytical models for both kinds of structures were proposed, in order to describe their resonant extinction cross-section behavior in terms of wavelength position, magnitude and bandwidth.

Good agreement among analytical models, numerical results and experimental values existing in literature was achieved.

By using the proposed models, the effects of the geometrical and electromagnetic parameters on the nanoparticles resonant properties were studied.

Finally, the structures were analyzed in terms of sensitivity properties, in order to verify the possibility to use them as sensing platform in the visible and infrared frequency regime for biomedical applications.

In particular, analytical, numerical and experimental results clearly demonstrated and confirmed the high sensitivity properties of the proposed modified bow-tie particles.

REFERENCES

[1] A. Moores and F. Goettmann, "The Plasmon Band in Noble Metal Nanoparticles: An Introduction to Theory and Applications," *New Journal of Chemistry*, Vol. 30, No. 8, 2006, pp. 1121-1132. doi:10.1039/b604038c

[2] W. Cai, T. Gao, H. Hong and J. Sun, "Applications of Gold Nanoparticles in Cancer Nanotechnology," *Nanotechnology*, *Science and Applications*, Vol. 1, 2008, pp. 17-32.

[3] J. C. Riboh, A. J. Haes, A. D. McFarland, C. Ranjit and R. P. Van Duyne, "A Nanoscale Optical Biosensor: Real Time Immunoassay and Nanoparticle Adhesion," *The Journal of Physical Chemistry B*, Vol. 107, No. 8, 2003, pp. 1772-1780. doi:10.1021/jp022130v

[4] J. J. Storhoff, R. Elghanian, R. C. Mucic, C. A. Mirkin

and R. L. Letsinger, "DNA Directed Synthesis of Binary Nanoparticle Network Materials," *Journal of American Chemical Society*, Vol. 120, No. 48, 1998, pp. 12674-12675. doi:10.1021/ja982721s

[5] E. M. Larsson, J. Alegret, M. Kall and D. S. Sutherland, "Sensing Characteristics of NIR localized Surface Plasmon Resonances in Gold Nanoring for Application as Ultrasensitive Biosensors," *Nano Letters*, Vol. 5, No. 5, 2007, pp. 1256-1263. doi:10.1021/nl0701612

[6] R. Bukasov, T. A. Ali, P. Nordlander and J. S. Shumaker-Parry, "Probing the Plasmonic Near-Field of Gold Nanocrescent Antennas," *ACS Nano*, Vol. 4, No. 11, 2010, pp. 6639-6650. doi:10.1021/nn101994t

[7] W. J. Galush, S. A. Shelby, M. J. Mulvihill, A. Tao, P. Yang and J. T. Groves, "A Nanocube Plasmonic Sensor for Molecular Binding on Membrane Surfaces," *Nano Letters*, Vol. 9, No. 5, 2009, pp. 2077-2082. doi:10.1021/nl900513k

[8] H. M. Hiep, T. Endo, K. Kerman, M. Chikae, D.-K. Kim, S. Yamamura, Y. Takamura and E. Tamiya, "A Localized Surface Plasmon Resonance Based Immunosensor for the Detection of Casein in Milk," *Science and Technology of Advanced Materials*, Vol. 8, No. 4, 2007, pp. 331-338. doi:10.1016/j.stam.2006.12.010

[9] D. Yelin, D. Oron, S. Thiberge, E. Moses, Y. Silberberg and I. Willner, "Multiphoton Plasmon-Resonance Microscopy," *Optics Express*, Vol. 11, No. 12, 2003, pp. 1385-1391. doi:10.1364/OE.11.001385

[10] K. Sokolov, M. Follen, J. Aaron, I. Pavlova, A. Malpica, R. Lotan and R. Richards-Kortum, "Real-Time Vital Optical Imaging of Precancer Using Anti-Epidermal Growth Factor Receptor Antibodies Conjugated to Gold Nanoparticles," *Cancer Research*, Vol. 63, No. 9, 2003, pp. 1999-2004.

[11] M. Y. Sham, H. Xu and R. Cromer, "SERS Nanoparticles: a New Optical Detection Modality for Cancer Diagnosis," *Nanomedicine*, Vol. 2, No. 5, 2007, pp. 725-734. doi:10.2217/17435889.2.5.725

[12] L. Sun, C. Yu and J. Irudayaraj, "Raman Multiplexers for Alternative Gene Splicing," *Analytical Chemistry*, Vol. 80, No. 9, 2008, pp. 3342-3349. doi:10.1021/ac702542n

[13] X. Huang, P. K. Jain, I. H. El-Sayed and M. A. El-Sayed, "Plasmonic Photothermal Therapy (PPTT) Using Gold Nanoparticles," *Lasers in Medical Science*, Vol. 23, No. 3, 2008, pp. 217-228. doi:10.1007/s10103-007-0470-x

[14] P. K. Jain, K. S. Lee, I. H. El-Sayed and M. A. El-Sayed, "Calculated Absorption and Scattering Properties of Gold Nanoparticles of Different Size, Shape, and Composition: Applications in Biological Imaging and Biomedicine," *Journal of Physical Chemistry B*, Vol. 110, No. 14, 2006, pp. 7238-7248. doi:10.1021/jp057170o

[15] W. Ding, R. Bachelot, S. Kostcheev, P. Royer and R. E. de Lamaestre, "Surface Plasmon Resonances in Silver Bowtie Nanoantennas with Varied Bow Angles," *Journal of Applied Physics*, Vol. 108, No. 12, 2010, pp. 124314. doi:10.1063/1.3524504

[16] H. Fischer and O. J. F. Martin, "Engineering the Optical Response of Plasmonic Nanoantennas," *Optics Express*, Vol. 15, No. 12, pp. 9144-9154.

[17] Y. Zhao, N. Engheta and A. Alù, "Effects of Shape and Loading of Optical Nanoantennas on Their Sensitivity and Radiation Properties," *Journal of the Optical Society of America B*, Vol. 28, No. 5, 2011, pp. 1266-1274. doi:10.1364/JOSAB.28.001266

[18] C. Bohren and D. Huffmann, "Absorption and Scattering of Light by Small Particles," John Wiley, New York, 1983.

[19] P. B. Johnson and R. W. Christy, "Optical Constants of the Noble Metals," *Physical Review B*, Vol. 6, No.12, 1972, pp. 4370-4379. doi:10.1103/PhysRevB.6.4370

[20] J. G. Van Bladel, "Electromagnetic Fields," John Wiley & Sons, Hoboken, 2007. doi:10.1002/047012458X

[21] CST Computer Simulation Technology, www.cst.com.

[22] A. Weber-Bargioni, A. Schwartzberg, M. Schmidt, B. Harteneck, D. F. Ogletree, P. J. Schuck and S. Cabrini, "Functional Plasmonic Antenna Scanning Probes Fabricated by Induced-Deposition Mask Lithography," *Nanotechnology*, Vol. 21, No. 6, 2010, pp. 1-6. doi:10.1088/0957-4484/21/6/065306

[23] A. D. McFarland and R. P. Van Duyne, "Single Silver Nanoparticles as Real-Time Optical Sensors with Zeptomole Sensitivity," *Nano Letters*, Vol. 3, No. 8, 2003, pp. 1057-1062. doi:10.1021/nl034372s

[24] R. Morarescu, H. Shen, R. A. L. Vallée, B. Maes, B. Kolaric and P. Damman, "Exploiting the Localized Surface Plasmon Modes in Gold Triangular Nanoparticles for Sensing Applications," *Journal of Materials Chemistry*, Vol. 22, No. 23, 2012, pp. 11537-11542. doi:10.1039/c2jm30944k